Nuclear Instruments and Methods in Physics Research A 785 (2015) 201–205

Contents lists available at ScienceDirect

Nuclear Instruments and Methods in Physics Research A

journal homepage: www.elsevier.com/locate/nima

Technical Notes

In situ analysis of electrocrystallization process of metal electrodeposition with confocal energy dispersive X-ray diffraction based on polycapillary X-ray optics

Fangzuo Li [a,b,c], Zhiguo Liu [a,b,c], Tianxi Sun [a,b,c,*], Chaolin Yang [a,b,c], Weiyuan Sun [a,b,c], Xuepeng Sun [a,b,c], Yongzhong Ma [d], Xunliang Ding [a,b,c]

[a] The Key Laboratory of Beam Technology and Materials Modification of the Ministry of Education, Beijing Normal University, Beijing 100875, China
[b] College of Nuclear Science and Technology, Beijing Normal University, Beijing 100875, China
[c] Beijing Radiation Center, Beijing 100875, China
[d] Center for Disease Control and Prevention of Beijing, Beijing 100013, China

ARTICLE INFO

Article history:
Received 18 September 2014
Received in revised form
8 March 2015
Accepted 8 March 2015
Available online 16 March 2015

Keywords:
Polycapillary X-ray optics
Confocal energy dispersive X-ray diffraction
Electrocrystallization
In situ real-time analysis

ABSTRACT

The confocal energy dispersive X-ray diffraction (EDXRD) based on a polycapillary focusing X-ray lens (PFXRL) in excitation channel and a polycapillary parallel X-ray lens (PPXRL) in detection channel was presented to study the electrocrystallization process of metal electrodeposition. The input focal spot of the PPXRL and the output focal spot of the PFXRL was adjusted in a confocal configuration, and only the X-rays from the volume overlapped by the two foci could be accordingly detected by the detector. The experimental results demonstrated the confocal EDXRD could be used to in situ real-time analysis of electrochemical crystal growth process.

1. Introduction

Energy dispersive X-ray diffraction (EDXRD) as a powerful structural analytical technique is most frequently applied to crystalline materials, cultural heritage, biomedicine, life science and so on [1–7]. In recent years, the confocal technology based on polycapillary X-ray optics becomes popular [8–13], and confocal EDXRD expands its applications for micro X-ray diffraction analysis in the energy dispersive configuration [1,14–16]. This so-called confocal EDXRD technology is based on a polycapillary focusing X-ray lens (PFXRL) with a high gain in power density in the excitation channel and a polycapillary parallel X-ray lens (PPXRL) with a long input focal distance in the detection channel. This confocal configuration ensured the XRD signals only from the confocal micro-volume overlapped by the PFXRL and the PPXRL could be detected by the detector, which was helpful in improving the signal-to-noise ratio of the EDXRD spectra [1,16].

In situ time-resolved analysis approaches are important for material field, e.g., in situ monitoring the films growth process. A large number of literatures reported the use of EDXRD for in situ real-time investigating the growth and crystallization process of films [17–22]. For example, Jonas et al. [17] utilized the in situ EDXRD to monitor the formation of Cu(In,Ga)S_2(CIGS) films during reactive magnetron co-sputtering, and they found several effects, such as vapor pressure, substrate temperatures and so on, should been considered for deposition process. Also, the in situ time-resolved EDXRD approach has been used for investigating temporal changes in the bilayer structure upon hydration [23], sampling of the structural changes which occurring in the electrodic materials of a Li-ion cell during charge-discharge cycling [24], studying of a range of chemical syntheses [25], and so on.

Electrochemical metal deposition is a well-known oldest subject within the field of electrochemistry, and it takes place at electrode/electrolyte interfaces under the influence of an electric field. Metal electrodeposition contains the cathodic reduction of metal ions and electrocrystallization process, and always be used to change the surface properties of solid materials and/or preparation of metal materials with specific compositions and properties [26]. Electrocrystallization is the initial stage of electrodeposition. The nascent adsorbed metal atoms diffusion into the appropriate location (i.e., active sites) along the electrode surfaces and growth by incorporating into the lattice point, or formation of crystal nucleus and growth on the surface of electrode [27,28]. Electrocrystallization has always been intensively attracted researchers from physics, chemistry, and materials, as well as peers from industry, because of it determines not only

* Corresponding author at: College of Nuclear Science and Technology, Beijing Normal University, Beijing 100875, China. Tel.: +86 10 62207171.
E-mail address: stx@bnu.edu.cn (T. Sun).

http://dx.doi.org/10.1016/j.nima.2015.03.015
0168-9002/

the latter process of electrodeposition but also the structure and performance of the deposit [29]. Many approaches and techniques can be used for ex-situ and/or in situ exploring of the electrocrystallization process of metal electrodeposition, e.g., scanning electron microscope (SEM) [30], atomic force microscope (AFM) [31], transmission electron microscopy (TEM) [29], extended X-ray absorption fine structure (EXAFS) [32], angle dispersive X-ray diffraction (ADXRD) [33], grazing incidence X-ray scattering (GIXS) [34], electron backscattering diffraction (EBSD) [35], and so on. The objective of the present investigation was to conduct an in situ and real-time exploration of the electrocrystallization process of metal electrodeposition by utilizing the proposed confocal EDXRD. This confocal EDXRD has its advantages. For one thing, it is fast for the serials spectra collection allowing a very high density time sampling of the evolution of the electrocrystallization process of metal electrodeposition; for another, it need not any system components to be moved for the fixed diffraction angle, which makes the EDXRD setup more simplified. Finally, the important in situ time-resolved information about the phase formation and crystal growth of the electrocrystallization of copper electrodeposition were obtained with the confocal EDXRD technique.

2. Experiments

2.1. Materials preparation

An electrolytic cell was designed (Fig. 1). The cathode material was a chromium-iron alloy sheet and the anode material was a copper sheet. The cell was constructed of amorphous materials, scattering from which would contribute only to the background of the diffraction pattern. The cell was filled with 0.5 mol/L aqueous solution of $CuSO_4$, which was prepared by utilizing copper sulfate anhydrate (0.8 g) in distilled water (10 ml). The cathode electrode and the anode electrode was attached to the potentiostat. A reductive potential of -2 V was applied to the cathode electrode. The electrolyte solution was carefully de-aerated by argon bubbling before measurements. All experiments were performed at room temperature.

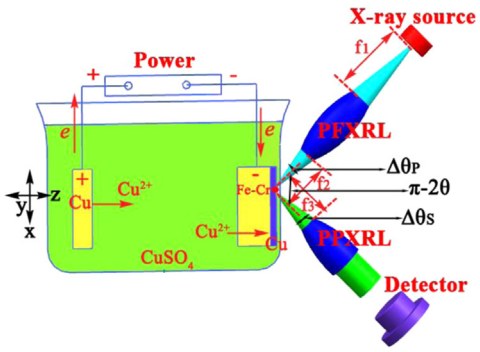

Fig. 1. Schematic diagram of the confocal EDXRD setup and electrolytic cell.

2.2. Confocal setup

Fig. 1 is the schematic diagram of the confocal EDXRD based on a PFXRL in the excitation channel and a PPXRL in the detection channel. The X-ray source was a Mo rotating anode X-ray generator with a spot size of $300 \times 300\ \mu m^2$. The operating voltage and current of the X-ray tube was 29 kV and 19 mA. The X-ray beam from the X-ray source positioned at a distance f_1 was focused by the PFXRL into its output focal spot with a distance f_2. The PPXRL at a distance f_3 was placed confocally with the PFXRL by using a liquid secondary target [36]. The profile size of the confocal micro-volume, overlapped by the output focal spot of the PFXRL and the input focal spot of the PPXRL, along the x, y and z direction (Fig. 1) was 50.2, 35.7 and 50.3 μm, respectively, at 17.4 keV. The parameters of the PFXRL and PPXRL are shown in Table 1. The detector system was an XFlash detector.

2.3. Confocal EDXRD

Basically physical theory background to EDXRD is well understood and described detail in Ref. [6]. The bremsstrahlung creates Laue diffraction peaks that originate from different crystallographic planes according to Bragg's condition, and has the following form:

$$2d \sin\theta = hc/E \tag{1}$$

where d is the lattice spacing, θ is the Bragg angle, E is X-rays energy, h is Planck's constant ($6.62606896 \times 10^{-34}$ J s), and c is the speed of light in vacuum (2.99792458×10^8 m s^{-1}). According to the Eq. (1), the resolution of lattice spacing $\Delta d/d$ of this confocal EDXRD diffractometer can be written as

$$(\Delta d/d)^2 = (\Delta\theta \cot\theta)^2 + (\Delta E/E)^2 \tag{2}$$

here, $\Delta E/E$ is relative energy resolution of the detector system and $\Delta E/E = 0.142/5.9 = 0.024$ at 5.9 keV. The angular resolution $\Delta\theta$ can be calculated with $\Delta\theta_p$ and $\Delta\theta_s$ from Fig. 1 as

$$\Delta\theta^2 = \Delta\theta_p^2 + \Delta\theta_s^2 \tag{3}$$

where $\Delta\theta_p$ is the convergence angle of the PFXRL and$\Delta\theta_s$ is the divergence angle of the PPXRL. The values of $\Delta\theta_p$ and $\Delta\theta_s$ were 82.5 and 81.3 mrad, respectively, at 5.9 keV. For this confocal EDXRD setup, θ was fixed as 48°. Therefore, the geometric resolution is $\Delta\theta \cot\theta = 0.104$, and the lattice spacing resolution of this confocal EDXRD diffractometer is 0.107 at 5.9 keV. From the values of $\Delta E/E$, $\Delta\theta\cot\theta$, and $\Delta d/d$, it can be seen that the geometric resolution $\Delta\theta\cot\theta$ is the dominating component of the total resolution $\Delta d/d$. For higher energy E, this statement is also correct, though the convergence $\Delta\theta_p$ and the divergence $\Delta\theta_s$ were decrease with higher energies [4,12,16], whilst the relative energy resolution $\Delta E/E$ of a silicon detector was decreased with increasing energies [1,37].

Table 1
Parameters of the PFXRL and PPXRL.

Lens	PFXRL	PPXRL
Length (mm)	73.4	20.3
Input focal distance (f_1 and/or f_3) (mm)	101.9	15.3
Output focal distance (f_2) (mm)	14.2	Not available
Diameter of IFS at 17.4 keV/μm	196.7	30.6
Diameter of OFS at 17.4 keV/μm	31.5	Not available
The convergence and/or divergence angle at 5.9 keV (rmad)	82.5	81.3
Gain in power density at output focal spot at 17.4 keV	3010	7